Quantitative Collection and Enzymatic Activity of Glucose Oxidase Nanotubes Fabricated by Templated Layer-by-Layer Assembly

Supporting Information

Shouwei Zhang, Sophie Demoustier-Champagne* and Alain M. Jonas*

Institute of Condensed Matter and Nanosciences - Bio and Soft Matter (IMCN/BSMA), Université catholique de Louvain, Croix du Sud 1/L7.04.02, B1348 Louvain-la-Neuve, Belgium

(*) Email : sophie.demoustier@uclouvain.be

(*) Email : alain.jonas@uclouvain.be

SEM image of the membrane before and after LbL templating, and STEM images of liberated nanotubes showing the presence of an open channel in the tubes.

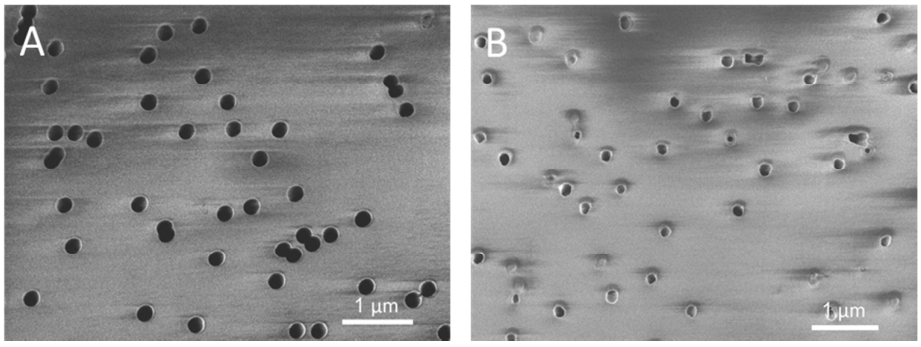

Figure S1a. SEM micrographs **(A)** of a virgin track-etched polycarbonate membrane as used in this work; **(B)** of a membrane containing $(bPEI/GOX)_6$ nanotubes, after surface decrusting.

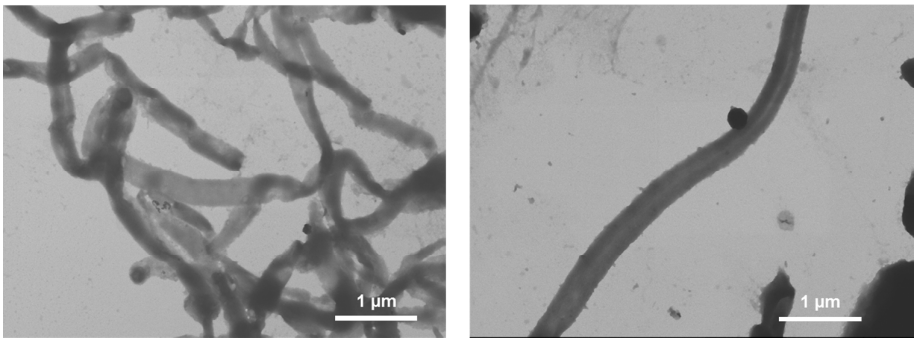

Figure S1b. STEM images of nanotubes showing their hollow core, even though they are collapsed after collection.

Preparation of samples for STEM measurements – ice collection route

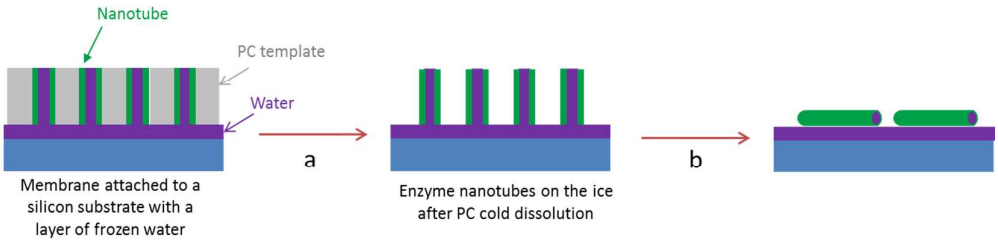

Scheme S1. Schematic illustration of the liberation process of enzyme nanotubes from a PC template for STEM observation, using an ice collection route. (a) Cold dissolution of the PC framework in CH_2Cl_2. (b) Ice melting at room temperature. The tubes are subsequently transferred to a TEM grid.

FTIR fitting procedure

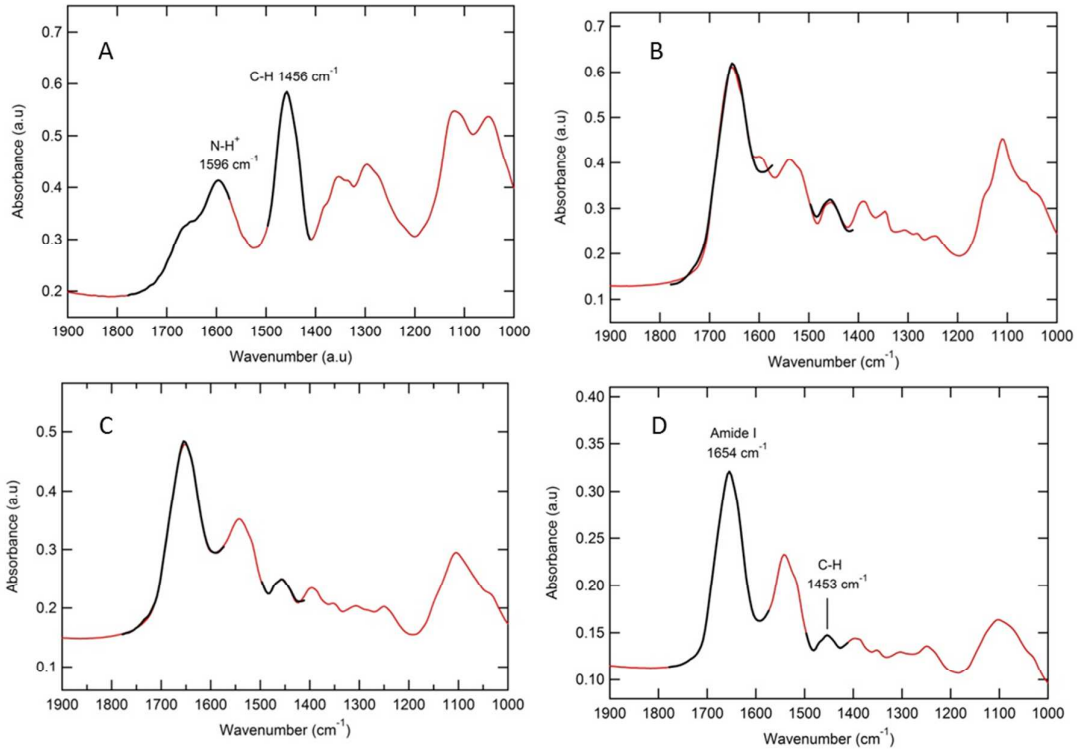

Figure S2. Fits (black lines) of the raw spectra of bPEI/GOX mixtures (red lines) of precisely known compositions. These analyses were performed in order to obtain a calibration curve relating the composition by weight of the mixtures to the relative intensity of the components of their FTIR spectra. The fits were restricted to spectral regions in which the spectra vary linearly with respect to the contents in both bPEI and GOX. A, pure bPEI; B, W_{bPEI}:W_{GOX} = 1:2.7; C, W_{bPEI}:W_{GOX} = 1:4; D, pure GOX.

Table S1. Fitting results from the FTIR spectra of mixtures measured for the calibration

W_{bPEI}/W_{GOX}	1	0.5	0.4	0.37	0.333	0.25	0.2	0.167	0.143	0.125	0.111	0.1
F_{bPEI}/F_{GOX}	0.221	0.114	0.102	0.091	0.079	0.058	0.044	0.039	0.035	0.026	0.020	0.016

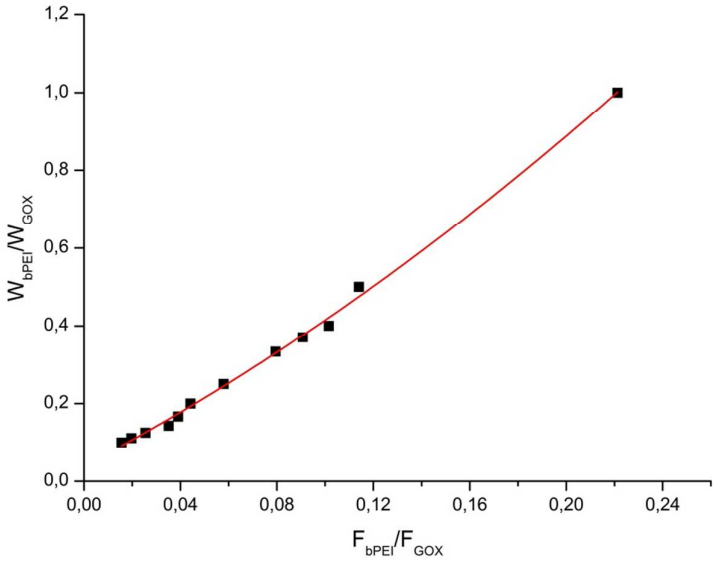

Figure S3. FTIR calibration curve from Table S1; the red line is :

$$W_{bPEI}/W_{GOX}\ (w{:}w) = 0.03955 + 3.2588\ x + 4.9170\ x^2, \text{ where } x = F_{bPEI}/F_{GOX}.$$

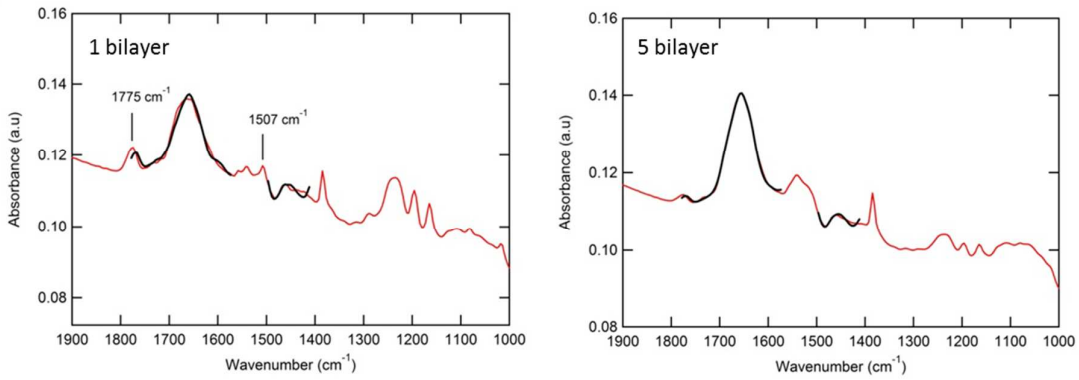

Figure S4. Typical fits of the raw spectra of nanotubes with different numbers of bilayers fabricated in 10 mM buffer (HEPES), pH 7.0. The signal of GOX dominates the spectra.

Table S2. Fitting results and calculated ratio by weight of bPEI to GOX in nanotubes prepared in 10 mM HEPES buffer (pH 7.0).

Number of bilayers	F_{bPEI}/F_{GOX}	W_{bPEI}/W_{GOX}
4	0.058	**0.25**
5	0.035	**0.16**
6	0.048	**0.21**
7	0.049	**0.21**
8	0.040	**0.18**
9	0.053	**0.23**

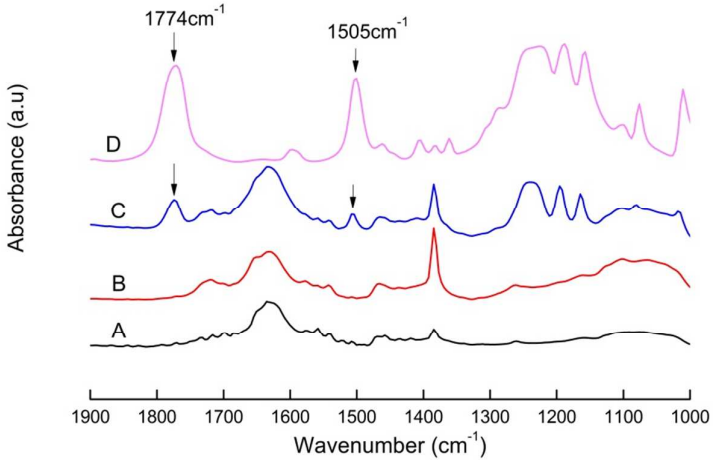

Figure S5. FTIR spectra of (A) pure KBr, (B) KBr powder after filtration of CH_2Cl_2, and (C) KBr powder after filtration of pure PC in CH_2Cl_2, (D) pure PC; these spectra demonstrate the trend of PC to adsorb on KBr from CH_2Cl_2.

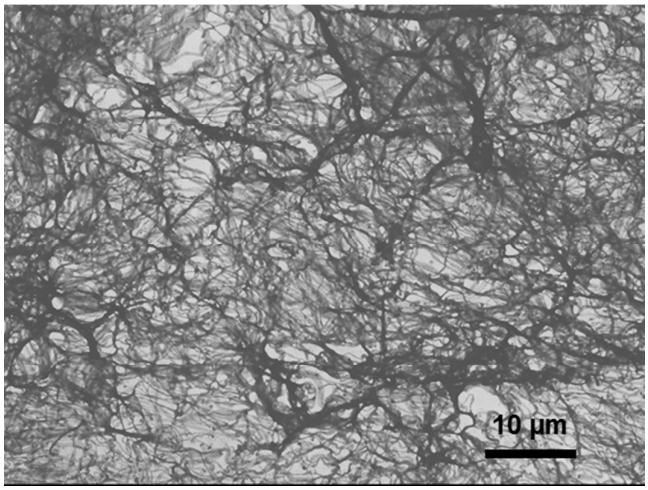

Figure S6. STEM image of a thin but dense film of nanotubes prepared using the ice collection route (Scheme S1), then transferred to a TEM grid.

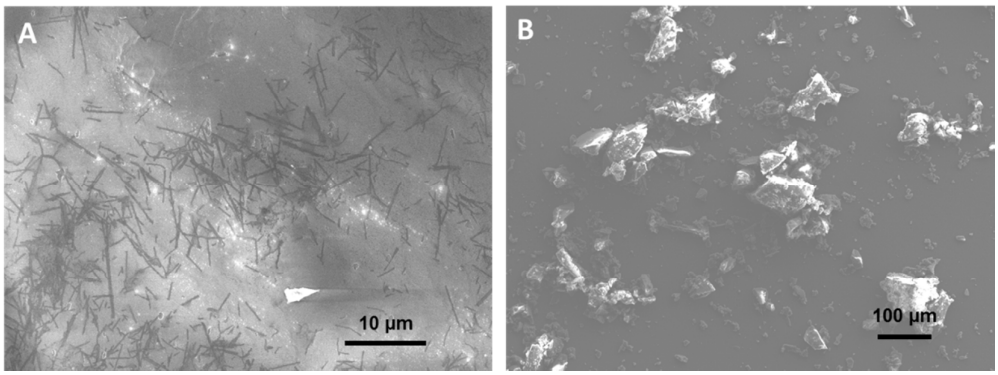

Figure S7. Microscopy images of nanotubes (A) on the filter after removal of the adjuvant cake when fructose of large powder size (B) is used in the fabrication of the barrier cake layer.

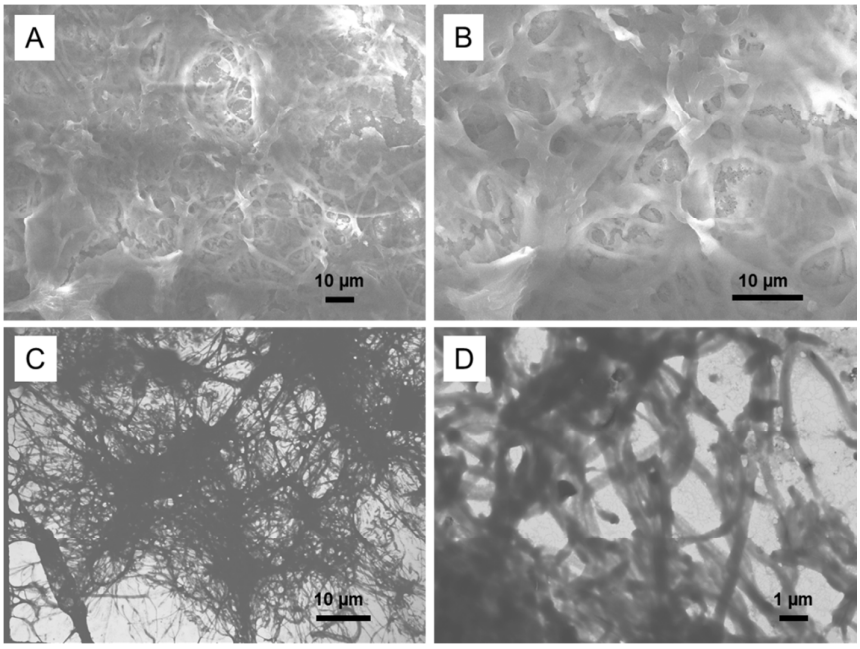

Figure S8. SEM (A,B) and STEM (C,D) images of clusters of nanotubes formed over the adjuvant barrier cake when the adjuvant powder is not added to the CH_2Cl_2 suspension of nanotubes in the second step of the collection procedure. The adjuvant is finely-ground fructose.

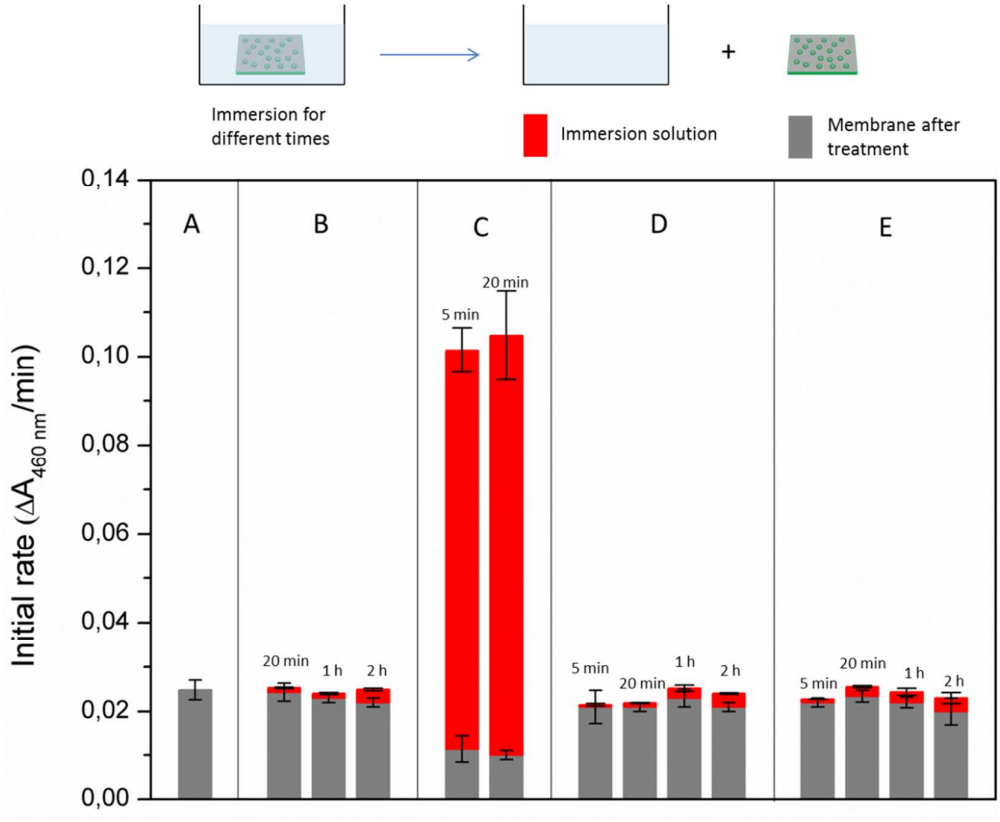

Figure S9. Investigation of the effect of adjuvants on the stability of 6-bilayer nanotubes embedded in the templates, by measuring the activity of the membranes (A) before and after immersion of the membrane in (B) 50 mM sodium acetate buffer, pH 5.5, (C) 45 mg NaCl in 2 mL of 50 mM sodium acetate buffer, pH 5.5, (D) 45 mg dextran in 2 mL of 50 mM sodium acetate buffer, pH 5.5, and (E) 45 mg fructose in 2 mL of 50 mM sodium acetate buffer, pH 5.5, for times varying from 5 min to 2h. The activities of the immersion solutions after removal of the membranes were tested as well, and are shown in red.

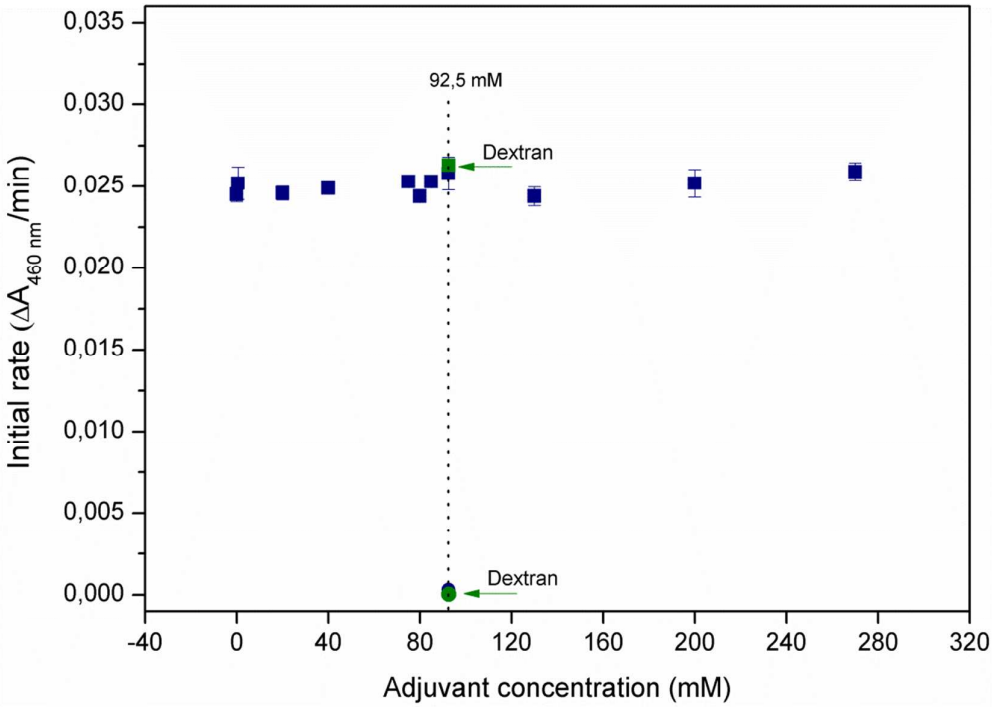

Figure S10. Effect of the presence of the adjuvants (fructose, full blue squares; or dextran, full green squares) on the activity towards glucose of free GOX in solution. The full circles indicate the activity towards either dextran (green) or fructose (blue), in the absence of glucose. Activities were tested by following a protocol identical to the one used for nanotube-embedded membranes, with a GOX and glucose concentration in the cuvette of 0.925 µg/ml and 0.56 mM, respectively (except for the full circles, for which no glucose but 0.5 ml of H_2O was added in the cuvette). The vertical dotted line at 92.5 mM adjuvant corresponds to the final concentration of adjuvant in the cuvette, for our other experiments measuring the activity of suspensions of freed nanotubes. For dextran, the molarity was computed from the molar mass of the repeat unit (glucose, 180 g/mol).

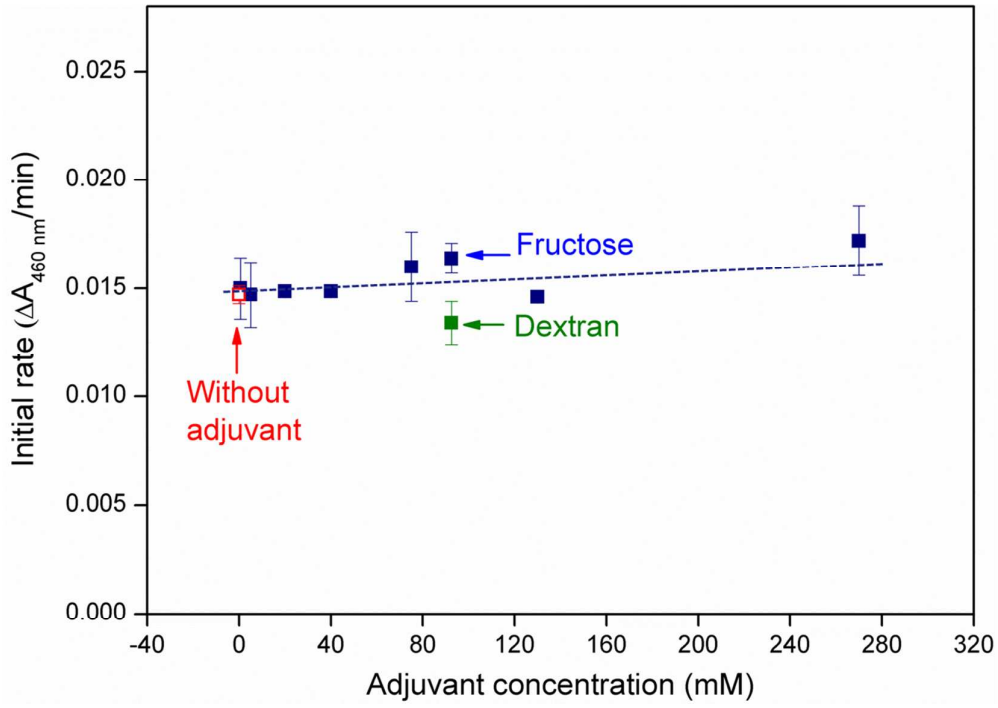

Figure S11. Effect of the presence of an adjuvant (fructose, full blue squares; dextran, full green squares) on the activity of flat $(GOX/bPEI)_{6.5}$ LbL films prepared in 10 mM HEPES buffer, pH 7.0, throughout. The red open square is the activity of this flat film towards glucose in the absence of added adjuvant. The dry thickness of the 6.5-bilayer films was approximately 35 nm, as measured by ellipsometry. The dotted line is drawn to guide the eye.

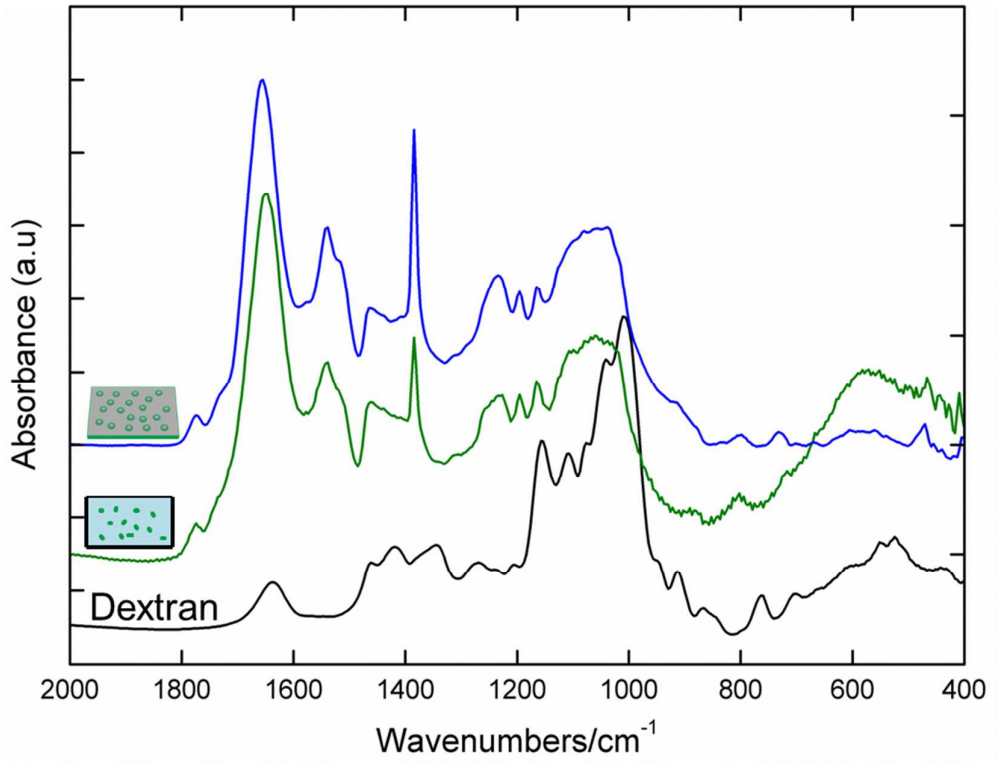

Figure S12. FTIR spectra of pure dextran (black solid line), 6.5-bilayer nanotubes extracted directly from PC template (blue solid line), and the same collected in aqueous suspension with dextran as adjuvant (green solid line).